

Effects of surface area, polymer char, oxidation, and NiO additive on nitridation kinetics of silicon powder compacts

R. T. BHATT

Vehicle Technology Center, U.S. Army Research Laboratory, Lewis Research Center, Cleveland, OH 44235, USA

A. R. PALCZER

National Aeronautics and Space Administration, Lewis Research Center, Cleveland, OH 44135, USA

E-mail: Ramakrishna.T.Bhatt@lerc.nasa.gov

The oxidative stability of attrition-milled silicon powder under reaction-bonding processing conditions has been determined. The investigation focused on the effects of surface area, polymer char, preoxidation, nitriding environment, and a transitional metal oxide additive (NiO) on the nitridation kinetics of attrition-milled silicon powder compacts tested at 1250 and 1350 °C for 4 h. Silicon powder was wet-attrition-milled from 2 to 48 h to achieve surface areas (SAs) ranging from 1.3 to 63 m²/g. A silicon powder of high surface area (63 m²/g) was exposed for up to 1 month to ambient air or for up to 4 days to an aqueous-based solution with the pH maintained at 3, 7, or 9. Results indicated that the high-surface-area silicon powder showed no tendency to oxidize further, whether in ambient air for up to 1 month or in deionized water for up to 4 days. After a 1-day exposure to an acidic or basic solution, the same powder showed evidence of oxidation. As the surface area increased, so did the percentage nitridation after 4 h in N₂ at 1250 or 1350 °C. Adding small amounts of NiO significantly improved the nitridation kinetics of high-surface-area powder compacts, but both preoxidation of the powder and residual polymer char delayed it. Conversely, the nitridation environment had no significant influence on the nitridation kinetics of a high-surface-area powder. Impurities present in the starting powder, and those accumulated during attrition milling, appeared to react with the silica layer on the surface of silicon particles to form a molten silicate layer, which provided a path for rapid diffusion of N₂ and enhanced the nitridation kinetics. © 1999 Kluwer Academic Publishers

1. Introduction

Reaction-bonded silicon nitride (RBSN) has long been considered a candidate material for hot-section structural components in advanced heat engine applications [1, 2]. This material is typically fabricated by first consolidating 3- to 50- μm sized commercially available silicon powders into a desirable shape. Then the shaped object is nitrided between 1350 and 1450 °C in N₂(g) or in a N₂-H₂(g) environment for 50 to 100 h [3]. The main attributes of RBSN are ease of fabrication, near net shape capability, high creep resistance, high-temperature strength, and low density. In spite of these advantages, RBSN is not used for commercial applications because of its low fracture strength at room temperature, low fracture toughness, and high internal oxidation rates between 800 and 1000 °C. Although its strength properties can be improved by controlling the processing variables and post-fabrication treatments [4], and its internal oxidation problems can

be alleviated by chemically vapor depositing a dense layer of Si₃N₄ or by infiltrating the porous body with a Si₃N₄-yielding polymer [5, 6], its fracture toughness cannot be altered to any perceptible degree by conventional processing methods. A possible way to solve this problem is to reinforce the RBSN with ceramic fibers. Previous studies have shown that strong and tough SiC/RBSN composites can be fabricated by reinforcing RBSN with 144- μm -diameter SiC fibers [7]. Although this composite has been used as a model system to study structure and property correlation, it cannot be used for high-temperature applications for two reasons: (1) it has limited shape capability because its large diameter fibers cannot be bent to a radius less than 12 mm; and (2) it is prohibitively expensive to machine complex-shaped components from a composite block. Both of these problems can be overcome by choosing small diameter ($\sim 14 \mu\text{m}$) SiC fibers as a reinforcement.

Because of SiC fiber degradation [8], the traditional processing methodology and nitridation cycles used for monolithic RBSN cannot be utilized in the fabrication of small diameter SiC-fiber-reinforced RBSN composites. Also, fabrication of high-volume-fraction composites from commercially available silicon powders ranging in diameter from 3 to 50 μm is difficult, since interfiber distances are typically less than 1 μm in composites containing fiber fractions greater than 20%. Therefore, the fabrication of second generation RBSN composites with small diameter SiC fibers requires the use of submicron silicon powders and a shorter, lower temperature nitridation cycle that is benign to commercially available SiC fibers.

Submicron silicon powders have been processed by a variety of processing routes; namely, laser synthesis of silane and hydrogen [9], and attrition or jet milling of commercially available silicon powders [10]. Sheldon and Haggerty [11] have reported that very high purity submicron-sized silicon powders have a tendency to agglomerate and are difficult to disperse in the organic liquids typically used in RBSN processing. They also showed that laser-synthesized, very high purity submicron-sized silicon powders having no (or only a fractional monolayer of) silica are prone to oxidation during air exposure and in contact with many of the polymer binders used in processing RBSN. In addition, they reported that oxidation of these powders can delay or even completely stop the nitridation reaction, depending on the degree of oxidation. Thus, these powders should be handled in an inert environment until nitridation, which imposes severe restrictions on their use for industrial-scale processing. On the other hand, the oxidative stability and the nitridation kinetics of submicron silicon powder obtained by milling commercially available silicon powder are not fully understood.

The objectives of this study were several: first, to determine the influence of surface area on the nitridation kinetics of attrition-milled silicon powder compacts; second, to study the oxidative stability of high-surface-area powders in ambient air and under RBSN processing conditions, which includes exposure to aqueous-based solutions and polymeric binders; and third, to determine the effects of carbon char, preoxidation nitridation environment, and a nitride-enhancing additive (NiO) on the nitridation kinetics of high-surface-area powder compacts.

2. Experimental procedure

Commercial silicon powder (Sicomill grade-IV supplied by Kemanord, Ljungaverk, Sweden) was used for this study. The as-received silicon powder was attrition-milled to reduce its particle size and, hence, to increase its surface area. A silicon nitride grinding medium was used to carry out the milling at room temperature for 2, 8, 32, and 48 h, with Stoddard (kerosene-based fluid) as the grinding fluid. The weight ratio of silicon powder to grinding medium was ~ 40 . The attrition milling was accomplished by using the procedure detailed in [10]. Afterwards, the excess grinding fluid was siphoned off

from the grinding vessel. Then, the silicon slurry was poured into a rectangular pan and dried for 24 h in a vacuum oven set at 600 $^{\circ}\text{C}$. The dried powder was transferred to a glass jar and stored in a glovebox that was purged continuously with high purity nitrogen.

The impurities in and particle size range and specific surface area of the silicon powders were determined, respectively, by wet chemistry, laser light scattering (Microtrac, Model 7991), and three-point Brunauer-Emmett-Teller (BET) adsorption (Micromeritics, Model ASAP 2010) techniques.

Some batches of the 48-h-attrition-milled silicon powders were exposed to ambient air for 1 h, or for 1, 7, or 30 days. Other batches were exposed to water-based solutions maintained at a pH of 3, 7, or 9 for 1 or 4 days. The pH of the solutions was adjusted with sulfuric acid or ammonium hydroxide. After exposure the powders were thoroughly rinsed with deionized water until no acidic or basic residue remained on the surface of the powder.

The silicon compacts, 12.7 mm in diameter and 2 to 3 mm thick, were prepared by uniaxially pressing attrition-milled silicon powder in a stainless steel die at 70 MPa. The compacts were $\sim 45\%$ dense compared to the theoretical density of silicon (2.33 g/cm^3). To determine the influence of carbon char on nitridation kinetics, the 48-h-attrition-milled silicon powders were blended with 15 wt % polybutyl methyl acrylate (PBMA, Aldrich Chemical Co. Milwaukee, WI) or with 10 wt % carbon black with an SA of 360 m^2/g (Regal 330 GP3094, Cabot Corporation, Waltham, MA).

The silicon compacts were nitrided for 4 h at 1250 or 1350 $^{\circ}\text{C}$ in a thermogravimetric analysis unit (Netzsch, Model 429/409) equipped with a tungsten-element furnace. The nitriding atmospheres were flowing N_2 (99.999 wt %), $\text{N}_2 + 4\% \text{H}_2$ (99.99 wt %), or $\text{N}_2 + 5\% \text{NH}_3$ (99.99 wt %). These gases were percolated through several cartridges of gettering agents to reduce oxygen and water vapor content to less than 10 ppm. After gettering, these gases typically contained 3 to 4 ppm of water vapor and oxygen.

Following nitridation, the compacts were analyzed for impurities and phase composition by wet chemistry and X-ray diffraction (XRD), respectively. Standard powder diffraction equipment with a nickel filter and $\text{CuK}\alpha$ radiation was used at a scanning speed of 1 deg/min for the XRD runs.

3. Results

The particle size, surface area, and impurity analysis of the as-received and 2-, 8-, 32-, and 48-h-attrition-milled silicon powders are shown in Tables I and II. According to Table I, the as-received silicon powder contained iron and oxygen as major impurities. As the attrition-milling time increased, the average particle size decreased and the surface area increased, as expected, but the amounts of yttrium, aluminum, and oxygen impurities also increased. The amount of yttrium and aluminum impurities varied with the attrition milling time and reached values of ~ 700 and 200 ppm, respectively, for the 48-h-attrition-milled powders. The source of these

TABLE I Particle size, surface area, and impurity analysis of as-received silicon powder

Average particle size (μm)	23.12
Surface area (m^2/g)	1.3
Impurities (wt %)	
Carbon	0.01
Iron	0.02
Oxygen	0.7
Impurities (ppm)	
Aluminum	0.002
Chromium	0.02
Nickel	0.006
Yttrium	0.002

TABLE II Particle size, surface area, and impurity analysis of attrition-milled silicon powders

Milling time (h)	Average particle size (μm)	Specific surface area (m^2/g)	Oxygen (wt %)	Yttrium content	Aluminum (ppm)
2	15.94	3.6	1.01	0.002 ppm	30
8	1.44	9.6	1.45	0.002 ppm	40
32	.54	30	3.71	0.06 wt %	120
48	.48	63	8.87	0.17 wt %	200

impurities was the Si_3N_4 grinding medium, which contained 6 wt % Y_2O_3 and 2 wt % Al_2O_3 as sintering additives.

3.1. Effect of air and solvent exposure on 48-h-attrition-milled silicon powder

Table III shows the oxygen content of the 48-h-attrition-milled silicon powder batches ($\text{SA} = 63 \text{ m}^2/\text{g}$) before and after exposure to ambient air for up to 1 month and to water-based solutions with the pH maintained at 3, 7, or 9 for up to 4 days. It is obvious from the table that the weight percent of oxygen present in the as-milled silicon powder exposed to air for up to 1 month or to deionized water for up to 4 days is similar to

TABLE III Oxygen content of 48-h-attrition-milled silicon powder ($\text{SA} = 63 \text{ m}^2/\text{g}$) exposed to air and to aqueous solutions

Exposure time (days)	Oxygen content (wt %)
As-milled	
0	7.70 ± 1.19
Dry air	
1/24	7.58
1	7.56
7	7.97
30	7.27
Deionized water; pH = ~7	
1	7.90
4	7.79
Acidic solution; pH = ~3	
1	6.4 ± 0.75
4	19.2
Basic solution; pH = ~9	
1	6.32 ± 0.53
4	15.8 ± 2.8

that of the unexposed as-milled powder. However the as-milled silicon powders exposed to acidic ($\text{pH} \sim 3$) and basic ($\text{pH} \sim 9$) solutions show higher oxygen values after a 4-day exposure than do the as-milled silicon powders.

3.2. Effect of surface area on nitridation kinetics

We determined the nitridation kinetics for compacts prepared from the as-received silicon powder and those attrition-milled for 2, 8, 32, and 48 h. The surface area of these powders, ranging from 1.3 to $63 \text{ m}^2/\text{g}$, depended on the attrition milling time. Fig. 1 shows typical nitridation behavior of the as-received powder and the powder attrition-milled for 8 or 48 h and nitrided in N_2 at 1250 or 1350 °C for 4 h. As the nitridation reaction progressed, the weight increased because silicon was converted to silicon nitride, but small amounts of silicon also evaporated as $\text{SiO}(\text{g})$ or $\text{Si}(\text{g})$, which resulted in weight loss. In the percentage nitridation plots shown in Fig. 1, the evaporation of these gaseous species during the reaction was not taken into account. It is clear from these figures that there are three regions of nitridation behavior: an induction period, a rapid nitriding period, and a nitridation saturation period. As the grinding time increased—in other words, as the surface area of the silicon powder increased—the slope of the second region and the percentage of silicon nitrided in 4 h also increased.

Fig. 2 shows how percentage nitridation varies with surface area for the silicon compacts nitrided at 1250 and 1350 °C for 4 h. Two main conclusions can be drawn from this figure: (1) as the surface area of the powder increases, the percentage of silicon converted

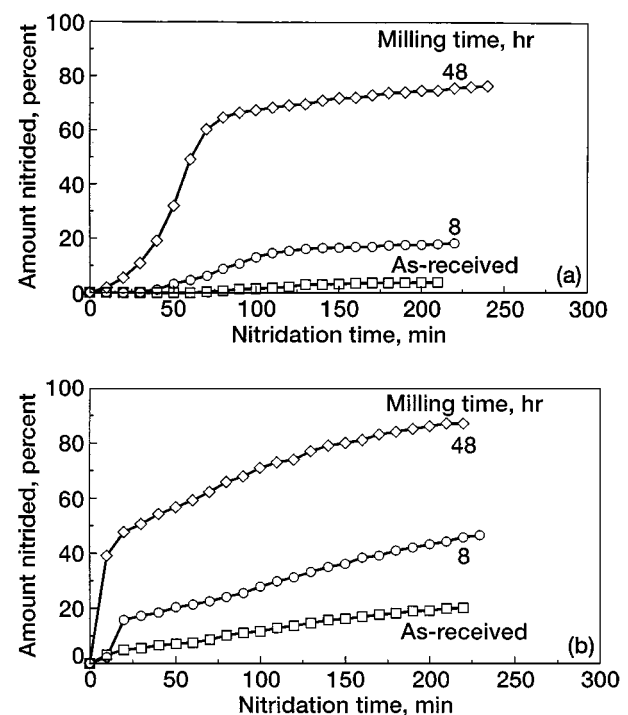


Figure 1 Nitridation behavior of as-received, and 8-h- and 48-h-attrition-milled silicon powder compacts ($\text{SA} = 1.3 \text{ m}^2/\text{g}$) nitrided in N_2 for 4 h (a) 1250 °C and (b) 1350 °C.

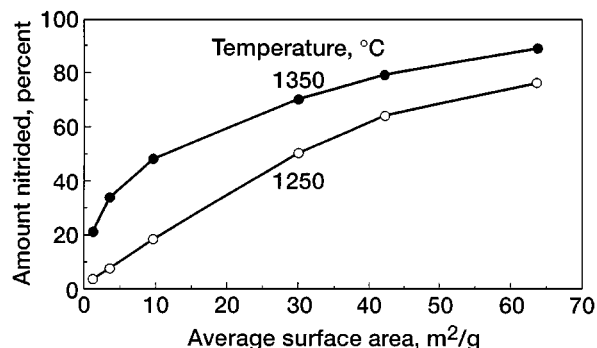


Figure 2 Variation of percent nitridation reaction with surface area for attrition-milled silicon powder compacts nitrided at 1250 and 1350 °C in N₂ for 4 h.

to silicon nitride also increases; (2) at the higher nitridation temperature the conversion rate is higher, especially for powders with a low surface area.

The phase and oxygen analysis of the nitrided as-received and attrition-milled silicon powder compacts are summarized in Tables IV and V. These tables clearly demonstrate that as the surface area increases the amounts of α -Si₃N₄ and β -Si₃N₄ in the compacts nitrided at each temperature increase continuously, but the ratio of α/β Si₃N₄ decreases, except in the case of the 63 m²/g silicon powder compact nitrided at 1350 °C. At a given nitridation temperature, the ratio of oxygen after nitridation to that before nitridation (referred to in the tables as the oxygen ratio) remains nearly the same with increasing surface area, but decreases with increasing temperature of nitridation. The compacts prepared from the highest surface area (63 m²/g) powder and nitrided at 1350 °C for 4 h contained an oxynitride phase and lower amounts of α -Si₃N₄ than the compacts prepared from most of the lower surface area powders nitrided under similar conditions. Tables IV and V also show that the total weight gain after the 4-h nitridation at each temperature also increased with increasing

TABLE IV Surface area effects on phase compositions and oxygen ratio of silicon compacts nitrided in N₂ at 1250 °C for 4 h

Surface area (wt %)	Si ₃ N ₄ (wt %)		α/β ratio	Unreacted silicon (wt %)	Oxygen ratio ^a	Weight gain (%)
	α	β				
1.3	3.7	0	—	96.3	0.71	0.80
3.6	6.7	1	6.7	92.2	0.63	3.60
9.6	12.3	6.2	2.1	81.5	0.79	10.04
30	26.3	24.3	1.08	49.4	0.76	23.08
63	40.1	36.6	1.09	23.4	0.72	32.12

^aRatio of oxygen after nitridation to oxygen before nitridation.

TABLE V Surface area effects on phase compositions and oxygen ratio of silicon compacts nitrided in N₂ at 1350 °C for 4 h

Surface area (m ² /g)	α -Si ₃ N ₄ (wt %)	β -Si ₃ N ₄ (wt %)	α/β ratio	Unreacted silicon (wt %)	Si ₂ N ₂ O (wt %)	Oxygen ratio ^a	Wt. gain (%)
1.3	18.6	2.8	6.64	78.6	0	0.6	6.80
3.6	26.8	7.1	3.77	66.1	0	0.59	13.70
9.6	34.2	14	2.44	51.7	0	0.67	26.48
30	34	36.5	0.93	29.5	0	0.68	34.20
63	9.1	73.5	0.12	10.7	6.8	0.67	36.10

^aRatio of oxygen after nitridation to oxygen before nitridation.

surface area. However, the maximum weight gain seen in the compacts nitrided to 90% or greater conversion is ~36 wt %, which is much lower than the theoretical value of 66 wt %. The discrepancy in the weight gain is partially due to the loss of silicon as SiO and silicon gas, and to the greater amounts of amorphous silica present in the finer powder, which did not nitride completely.

3.3. Effects of nitridation environment on nitridation kinetics

The influence of the nitridation environment (namely, N₂, N₂ + 4% H₂, or N₂ + 5% NH₃) on the nitriding kinetics of attrition-milled silicon powders (SAs = 9.6 and 63 m²/g) was investigated at 1250 and 1350 °C (Figs 3 and 4). The lower surface area powder was specifically chosen because the literature mentions the use of such powders for investigating the influence of the nitridation environment on nitridation kinetics. In general, adding H₂ or NH₃ to N₂ enhanced the nitridation kinetics of the low-surface-area powder, but had no significant influence on the high-surface-area powder. Results are summarized in Tables VI and VII for the

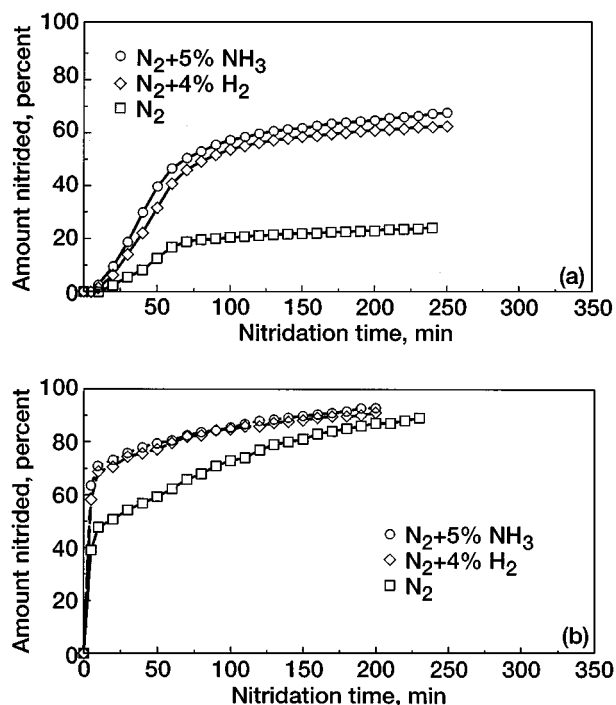


Figure 3 Influence of nitridation environment on nitridation kinetics of low-surface-area attrition-milled silicon powder compacts (SA = 9.6 m²/g) nitrided for 4 h (a) 1250 °C and (b) 1350 °C.

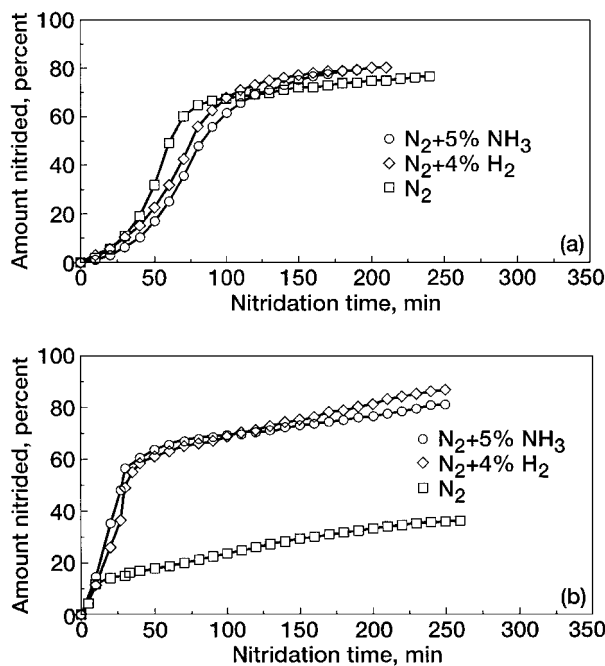


Figure 4 Influence of nitriding environment on nitriding kinetics of high-surface-area attrition-milled silicon powder compacts ($SA = 63 \text{ m}^2/\text{g}$) nitrided for 4 h (a) 1250°C and (b) 1350°C .

low- and high-surface-area powders, respectively. At a set nitriding temperature, the low-surface-area powder nitrided in N_2 yielded a consistently lower $\beta\text{-Si}_3\text{N}_4$ content than $\alpha\text{-Si}_3\text{N}_4$ content, and a lower α/β ratio than did the same powder nitrided in $\text{N}_2 + 4\% \text{H}_2$ or in $\text{N}_2 + 5\% \text{NH}_3$.

Conversely, the high-surface-area powder nitrided at 1250°C yielded nearly the same $\alpha\text{-Si}_3\text{N}_4$ content and α/β ratio irrespective of the nitriding environment. At 1350°C , the nitriding environment again had no effect, but the $\alpha\text{-Si}_3\text{N}_4$ content and α/β ratio were lower than those observed at 1250°C .

3.4. Effect of transitional metal impurities on nitriding kinetics

To understand the influence of transitional metal impurities on the nitriding kinetics, attrition-milled silicon powders having a nominal surface area of $\sim 63 \text{ m}^2/\text{g}$

TABLE VI Effects of nitriding environment and temperature on phase composition and oxygen ratio of nitrided 8-h-attrition milled silicon powder compacts ($SA = \sim 9.6 \text{ m}^2/\text{g}$)

Nitriding environment	Si_3N_4 (wt %)		α/β ratio	Unreacted silicon (wt %)	Oxygen ratio ^a
	α	β			
At 1250°C					
N_2	17.5	6.9	2.54	75.6	0.90
$\text{N}_2 + 4\% \text{H}_2$	59.7	7.8	7.65	32.6	0.96
$\text{N}_2 + 5\% \text{NH}_3$	60.8	7.3	8.33	31.9	0.89
At 1350°C					
N_2	34.2	14.0	2.44	51.7	0.67
$\text{N}_2 + 4\% \text{H}_2$	48.3	38.4	1.26	13.3	0.79
$\text{N}_2 + 5\% \text{NH}_3$	52.7	28.4	1.86	19	0.82

^aRatio of oxygen after nitridation to oxygen before nitridation. Duration of nitridation = 4 h.

TABLE VII Effects of nitriding environment and temperature on phase compositions and oxygen ratio of nitrided 48-h-attrition-milled silicon powder compacts ($SA = \sim 63 \text{ m}^2/\text{g}$)

Nitriding environment	Si_3N_4 (wt %)		α/β ratio	Unreacted silicon (wt %)	$\text{Si}_2\text{N}_2\text{O}$ (wt %)	Oxygen ratio ^a
	α	β				
At 1250°C						
N_2	15.4	48.5	0.32	33.1	3.4	0.77
$\text{N}_2 + 4\% \text{H}_2$	15.5	58.0	0.27	19.7	6.8	0.83
$\text{N}_2 + 5\% \text{NH}_3$	14.7	57.5	0.26	20.7	7.1	0.93
At 1350°C						
N_2	9.1	73.5	0.12	10.7	6.8	0.66
$\text{N}_2 + 4\% \text{H}_2$	8.5	75.9	0.11	15.6	0	0.89
$\text{N}_2 + 5\% \text{NH}_3$	3.1	77.3	0.04	7.6	11.9	0.87

^aRatio of oxygen after nitridation to oxygen before nitridation. Duration of nitridation = 4 h.

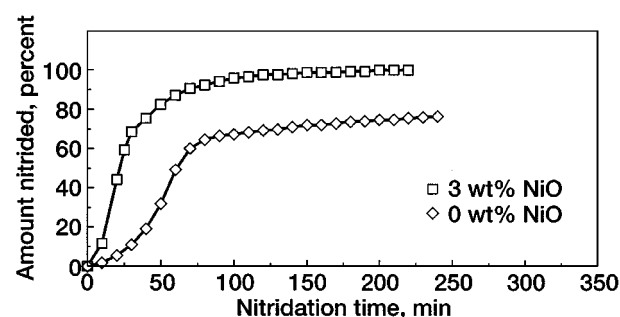


Figure 5 Nitriding behavior of 48-h-attrition-milled silicon powder compacts ($SA = 63 \text{ m}^2/\text{g}$) nitrided in N_2 with and without 3 wt % NiO (a) 1250°C and (b) 1350°C .

were blended with 0.5, 1.5, and 3.0 wt % NiO powder and pressed into pellets as usual; then they were nitrided at 1250 and 1350°C in nitrogen for 4 h. Fig. 5 depicts the typical nitriding behavior of compacts with and without 3 wt % NiO at 1250°C . Obviously, NiO-containing compacts show faster nitriding initially, but after 4 h the percentage nitridation is nearly the same as for those without NiO. Since the as-received silicon powder contained a small amount of iron impurities, and since iron is also known to enhance nitriding kinetics [3], the nitriding data of high-surface-area silicon powders containing different levels of NiO additive was plotted to reflect the combined effects of the iron and nickel impurities. Fig. 6 shows the

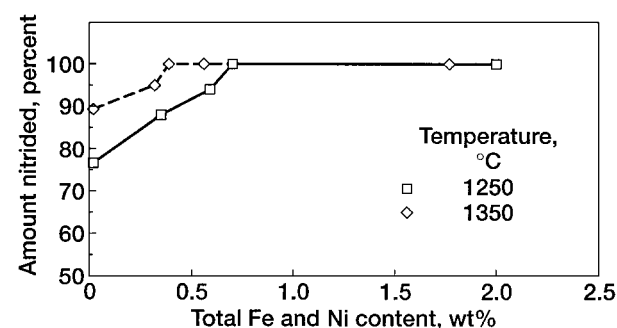


Figure 6 Variation of percent nitridation reaction with transitional metal impurity content for attrition-milled silicon powder compacts ($SA = 63 \text{ m}^2/\text{g}$) nitrided in N_2 at 1250 and 1350°C for 4 h.

percentage nitridation at 1250 and 1350 °C for compacts whose total iron and nickel impurities varied from 200 ppm to 3.0 wt %. This figure indicates that to fully nitride the silicon compacts at 1250 and 1350 °C, combined iron and nickel impurities of ~ 0.6 and ~ 0.4 wt %, respectively, are required. The phase analysis results of the NiO-containing compacts nitrided at 1250 and at 1350 °C indicate that their α -Si₃N₄ and β -Si₃N₄ contents are similar to those in compacts without NiO, under similar nitridation conditions. On the other hand, chemical analysis indicated an oxygen ratio of ~ 0.5 for compacts containing ~ 3 wt % NiO that were nitrided at 1250 °C, which is much lower than the 0.75 measured for compacts that contained no NiO but were nitrided at the same temperature. A similar trend was also noticed for compacts nitrided at 1350 °C with and without NiO.

3.5. Effect of carbon impurities on nitridation kinetics

Fugitive polymer binders are generally used in ceramic processing to facilitate consolidation of a ceramic powder. When ceramic powder compacts containing a polymer binder are heated in an inert environment, they leave small amounts of carbon char (<5 wt %) in the material. To evaluate the effect of carbon char and carbon on the nitridation kinetics, 48-h-atrition-milled silicon powder was mixed with 15 wt % PBMA binder or 10 wt % carbon black. Pyrolysis of the 15 wt % PBMA-containing powder at 500 °C in vacuum yielded ~ 2 wt % carbon char. To investigate the nitriding kinetics of silicon compacts containing the two different levels of carbon, the compacts were heated at 1250 or 1350 °C in nitrogen for 4 h. The results are shown in Fig. 7 along with the nitridation data previ-

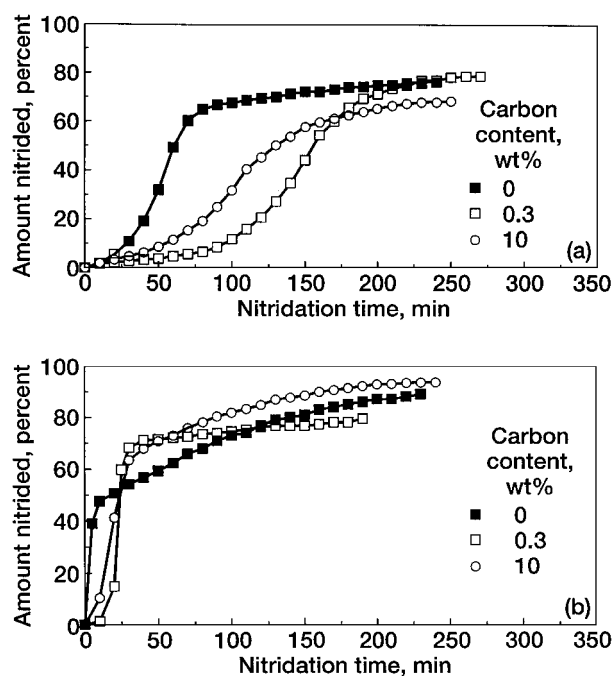


Figure 7 Nitridation behavior of 48-h-atrition-milled silicon powder compacts ($SA = 63 \text{ m}^2/\text{g}$) containing 0.3 wt % polymer char and 10 wt % carbon black nitrided in N₂ for 4 h (a) 1250 °C and (b) 1350 °C.

ously presented for the silicon powder compacts without carbon char. It appears from the data that carbon generally retards nitridation in the early stages. The type of carbon also appears to affect nitridation kinetics; the carbon char from the PBMA polymer delays the initiation of nitridation much more than carbon black does. However, after 4 h the percent nitridation with and without carbon char is nearly the same.

3.6. Effect of preoxidation on nitridation kinetics

Previous results showed that high-surface-area silicon powders are susceptible to further oxidation when exposed to acidic or basic solutions. To study the influence of oxidation on nitridation kinetics, the 48-h-atrition-milled silicon powder compacts ($SA = 63 \text{ m}^2/\text{g}$) without additives were first oxidized in air to 5 or 10 wt % gain to grow an additional layer of silica on the silicon. These compacts were nitrided in N₂ or in a N₂ + 4% H₂ mixture at 1250 and 1350 °C for 4 h; see Fig. 8. For comparison purposes, the figure also includes the nitridation kinetics of unoxidized silicon compacts. Clearly, as the degree of preoxidation increases, the incubation period for the start of the nitridation reaction also increases and the nitridation rate decreases. The nitridation rate of the 5%-oxidized compacts nitrided in N₂ was generally lower in the initial stages, but after 4 h, the percentage converted to Si₃N₄ reached a level similar to that of the unoxidized powder. The 10%-oxidized compacts, on the other hand, were only partially nitrided in N₂. In the N₂ + %H₂ environment, however, both the 5- and 10%-oxidized powder compacts were significantly nitrided, although the nitridation rate in the initial stages was slower. Neither the oxidation of the powder nor the addition of H₂ to the nitrogen had an appreciable effect on the α/β ratio of the nitrided compacts.

The influence of a nitride-enhancing additive on the nitridation kinetics of preoxidized silicon compacts similar to those just discussed was also investigated. Figure 9 shows the nitridation kinetics of preoxidized silicon powder compacts containing 3 wt % NiO at

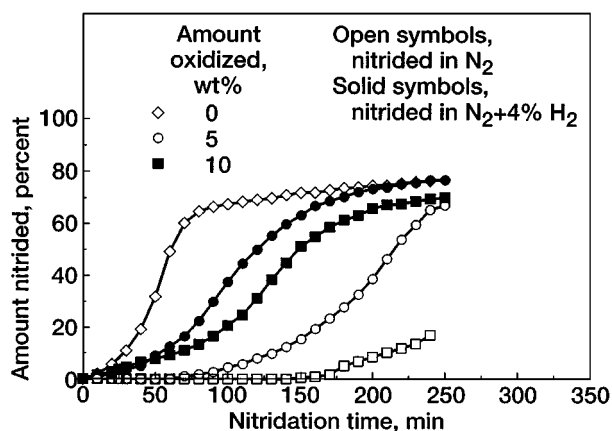


Figure 8 Influence of nitridation environment on 48-h-atrition-milled and preoxidized silicon powder compacts ($SA = 63 \text{ m}^2/\text{g}$) nitrided at 1250 °C for 4 h.

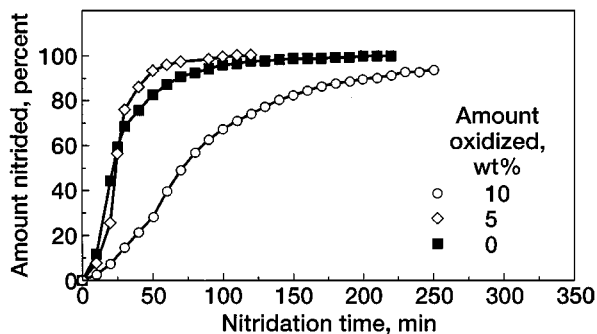


Figure 9 Effect of 3 wt% NiO additive on nitridation kinetics of 48-h-attribution-milled and preoxidized silicon powder compacts ($SA = 63 \text{ m}^2/\text{g}$) nitrided in N_2 at 1250°C for 4 h.

1250°C in N_2 , along with the nitridation data of an unoxidized compact containing the same additive. By comparing Figs 8 and 9, we see that the retardation of the nitridation reaction due to preoxidation can, to a great extent, be overcome by adding a nitridation-enhancing additive.

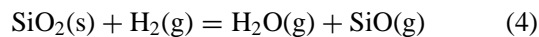
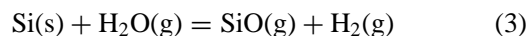
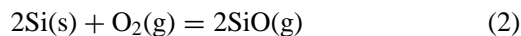
4. Discussion

According to Tables I and II, both the as-received and attrition-milled silicon powders contained iron (~ 200 ppm) as a major metallic impurity. Also, as the attrition-milling time increased, so did the specific surface area and the oxygen content of the powder. From this, we can conclude that attrition-milled silicon powders are partially oxidized and contain a native silica layer on their surfaces. Furthermore, with increased milling time, the wear of the Si_3N_4 milling medium caused extraneous impurities such as yttrium and aluminum to accumulate in the silicon powder.

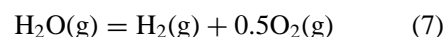
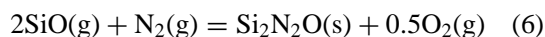
Although the 48-h-attribution-milled powders have a high surface area ($63 \text{ m}^2/\text{g}$), they do not appear to readily oxidize in ambient air. From a practical point of view, these data suggest that such powders can be stored for a long time without further oxidization. After prolonged exposure in aqueous-based slurries, however, these powders show a tendency to oxidize further. This suggests that these slurries have a limited shelf life. Insofar as nitridation is concerned, the silica layer on silicon powder is known to act as a barrier. Unless this layer is removed or disturbed, nitridation may not start.

The mechanism of nitridation and the effects of the nitridation environment and the transition metal impurities on the nitridation kinetics of relatively pure silicon powder containing a thin ($< 3 \text{ nm}$) native surface silica layer are reasonably well understood [3, 12–14]. Both thermodynamic analysis [3, 14] and experimental data [12, 13] indicate that nitridation occurs by gas phase reactions, largely between $\text{SiO}(\text{g})$ and $\text{N}_2(\text{g})$ and to a lesser extent between $\text{Si}(\text{g})$ and $\text{N}_2(\text{g})$. It has been postulated that during formation of RBSN the major growth of $\alpha\text{-Si}_3\text{N}_4$ occurs by vapor phase reactions and that of $\beta\text{-Si}_3\text{N}_4$ occurs in the liquid phase and, to a minor extent, as a result of the reaction between the solid silicon and nitrogen. Relevant details of this mechanism will be described here and used in later sections to explain the nitridation data generated in this study. According to

accepted models, nitridation starts with devitrification of the silica layer and a reaction between the silica layer and silicon that results in $\text{SiO}(\text{g})$. The SiO subsequently reacts with N_2 to form either Si_3N_4 or a combination of Si_3N_4 and $\text{Si}_2\text{N}_2\text{O}$. The series of reactions that control nitridation are as follows:



or



The preceding equations indicate that the $\text{SiO}(\text{g})$ required for gas phase nitridation is generated by four likely reactions: silica reacting with silicon (Equation 1), and residual oxygen or moisture in the nitrogen reacting with silica and silicon to actively oxidize silicon (Equations 2 to 4). The thermodynamic analysis of Giridhar and Rose [14] showed that for the formation of $\text{Si}_2\text{N}_2\text{O}(\text{s})$ and $\text{Si}_3\text{N}_4(\text{s})$ in N_2 at 1250°C , oxygen partial pressures (P_{O_2}) of $< 10^{-5.4}$ and $< 10^{-6.5}$ atm, respectively, must be maintained in the reaction zone. At higher temperatures, even higher P_{O_2} requirements favor the nitridation reaction. Of the four equations controlling SiO pressure, calculations show that Equations 1 and 4 are the dominant ones. Equation 1 indicates that there is a theoretical maximum value of $\text{SiO}(\text{g})$, which primarily varies with nitridation temperature. Although SiO may also be generated from active oxidation of silicon, its concentration from this reaction is limited by the residual oxygen in the nitriding gas (< 5 ppm), which contributes minimally to $\text{SiO}(\text{g})$ formation. Therefore, it has been argued that the partial pressure of $\text{SiO}(\text{g})$ is not determined by residual O_2 or H_2O , but by the devitrification of $\text{SiO}_2(\text{s})$ to form $\text{SiO}(\text{g})$ via Equation 1, and by the nitridation temperature via Equation 4. The most likely scenario for nitridation is that the $\text{SiO}_2(\text{s})$ layer reacts with $\text{Si}(\text{s})$ via Equation 1 and then with $\text{H}_2(\text{g})$ via Equation 4 to form $\text{SiO}(\text{g})$, thereby fixing the partial pressure of SiO at the nitridation temperature. As the nitridation temperature increases, the partial pressure of $\text{SiO}(\text{g})$ also increases, thus favoring the nitridation reaction. The SiO generated reacts with N_2 as shown in Equations 5 or 6. The oxygen liberated at this stage competes with nitrogen for the silicon surface exposed by the first reaction (Equation 1), severely limiting the nucleating sites for the nitridation reaction. Because nitridation occurs primarily by gas phase reactions, the α/β Si_3N_4 ratio observed was between 7 and 10 [3, 5, 11–13].

According to the preceding model, adding small amounts of H_2 to N_2 favors SiO nitridation even more. The O_2 generated by Equations 5 and 6 reacts with H_2

to form water and is thus removed and prevented from recombining with the exposed Si surface, which greatly enhances the extent of the reaction at lower temperatures. Thus H_2 plays a dual role in the nitridation of silicon: reduction of the native silica layer on silicon, and gettering the oxygen liberated during early stages of the nitridation reaction. The latter process keeps the surface of the silicon powder clear of silica for longer times, thus allowing the nitridation reaction to continue. On the basis of thermodynamic arguments alone, α - Si_3N_4 is favored over the oxynitride when hydrogen is present in the gas phase. The experimental data of Borsoum *et al.* [13], Rahaman and Moulson [15], and Mangels [16] strongly support the dual role played by hydrogen in enhancing nitridation kinetics.

An increase in the nitridation rate with the addition of a transitional metal oxide is well documented [17]. The addition of up to 1000 ppm of iron has been shown to increase the nitridation rate. A decreasing α/β ratio of Si_3N_4 with increasing iron has been found to be consistent with eutectic liquid formation in the Fe-Si system, which favors β - Si_3N_4 formation and an α - to β - Si_3N_4 transformation. The increased rate of nitridation has been attributed to three main factors: (1) devitrification of the inherent SiO_2 layer, possibly by providing nucleation sites for the devitrification process [18–22]; (2) formation of low-temperature silicide phases [3, 17] that provide alternate rapid nitrogen diffusion paths, which stimulate production of β - Si_3N_4 [17] and act as a source of volatile silicon (a precursor for one of the accepted mechanism of α - Si_3N_4 synthesis) [20]; and (3) promotion of the formation of atomic nitrogen as in catalysis of ammonia synthesis [23].

From the general mechanism of nitridation just described, we can analyze the effects of surface area, nitridation environment, polymer char, transitional metal impurities, and oxidation on the nitridation kinetics of attrition-milled silicon powders.

As stated previously, the attrition-milled silicon powder used contained a small amount (<0.02 wt %) of iron impurity. Only in a nitrogen environment does iron-induced crystallization of the native oxide layer occur, thereby exposing the underlying Si. After devitrification of the silica, nitridation is dictated by the rate of formation and growth of the Si_3N_4 nuclei. Here, particle size is a major influence. With decreasing particle size, the nominal surface area increases, which increases the nucleation sites per unit volume and promotes the conversion of Si to Si_3N_4 while reducing the influence of extraneous and intrinsic impurities on the nitridation kinetics.

The nitridation data show that the α/β ratio of the nitrided compacts decreases with increasing surface area at both nitriding temperatures, whereas the α - Si_3N_4 and β - Si_3N_4 content increases; however, in nitrided compacts containing Si_2N_2O , the α - Si_3N_4 content is much lower than the β - Si_3N_4 content.

Also noteworthy is that, at a given nitridation temperature, the ratio of oxygen in the compacts after and before nitridation is invariant with surface area, but it decreases with increasing temperature of nitridation. Recall from our earlier discussion that according to

Equation 1 SiO concentration in the reaction zone increases with the nitridation temperature. Therefore, an increase in percent nitridation for a given time and a decrease in oxygen ratio with an increase in nitridation temperature is probably related to SiO nitridation and reduction of the silica layer.

A decrease in the α/β ratio with an increase in surface area suggests that nitridation of powder compacts with lower surface area probably takes place primarily by gas phase reactions (i.e., SiO or Si reacting with N_2) and that nitridation of powders with higher surface area occurs by liquid phase reactions. A gradual change in the nitridation mechanism with increasing surface area is probably due to the accumulation of yttrium, and possibly aluminum, impurities and the reaction between these impurities and silica to form complex silicates. In the ternary phase diagram of Y_2O_3 , Al_2O_3 , and SiO_2 , the lowest liquidus temperature reported is $1345^\circ C$ [24]. Furthermore, the iron impurity may also react with the silica layer on the surface of the as-received and attrition-milled powders to form a liquid phase. It has been reported that the iron impurities in commercial grade silicon will form molten $FeSi_x$ at nitriding temperatures above $1207^\circ C$ [3, 17]. Although liquid phases may be a contributing factor to the enhanced diffusion of nitrogen, we cannot rule out the role played by increased surface area (decreased particle size), subsequent to attrition milling, in increasing the rate of formation and growth of Si_3N_4 nuclei. To determine the relative importance of liquid phases versus increased surface area (and thus, increased nucleation) effects on nitridation kinetics, compacts prepared from a blend of silicon powder ($SA = 9.3$ m^2/g) and 0.5 or 0.2 wt % Al_2O_3 were nitrided at $1350^\circ C$ in N_2 . The data were compared with the nitridation data of the compacts under similar conditions without the additives. Results showed that the liquid phase enhanced the nitridation kinetics initially, but the percentage conversion after 4 h of nitridation remained nearly the same; this indicates that a liquid phase without adequate nucleation and growth characteristics may not yield a high degree of conversion. Therefore, it can be concluded that surface area, and hence nuclei density per unit volume, plays a dominant role in the degree of conversion after the silica layer on the surface of silicon is disturbed.

Small additions (4 to 5%) of H_2 or NH_3 to nitrogen had a greater influence on the nitridation kinetics of lower surface area (9.3 m^2/g) attrition-milled powders than on those of higher surface area (63 m^2/g). The dramatic effects that small additions of H_2 made on the extent of the reaction are consistent with arguments suggesting that the gettering action of H_2 reduces the silica layer and creates new nucleation sites. The α - Si_3N_4 content of low-surface-area compacts nitrided in the $N_2 + 4\% H_2$ mixture was significantly higher than that of the compacts nitrided in N_2 alone. This suggests SiO nitridation is favored in lower surface area powders in the presence of H_2 . In contrast, the nitridation environment had little effect on the nitridation kinetics of high-surface-area powder compacts. Perhaps this behavior is related to the high density of Si_3N_4 nuclei and the faster diffusion of N_2 through the molten

complex silicates. These data are similar to those reported by Rahaman and Moulson [15] on the nitridation of silicon after removal of the silica layer.

The carbon char in silicon powder after polymer pyrolysis can serve three functions during the nitridation of silicon; two of these are similar to the action of H₂ (i.e., gettering of residual oxygen by forming CO or CO₂, and reduction of the silica layer on the surface of silicon), and the third is its possible reaction with silicon to form SiC once the silica layer is removed. The data, however, indicate that carbon char retards initiation of the nitridation reaction as well as nitridation kinetics. This behavior is probably related to a loss of nucleation sites or to the poisoning of active centers by carbon. The degree of retardation depends on the type of carbon: polymer derived carbon inhibits more than activated carbon does.

The intentional addition of NiO to high-surface-area silicon powder increases the nitridation rate. In such cases, compacts can be completely nitrided within 2 h at 1250 or 1350 °C. Certainly the liquid phase formed because of NiO, SiO₂, and other impurities plays a dominant role in the diffusion of nitrogen and in nitridation. The oxygen present in the compacts containing NiO that were nitrided at 1250 °C is less than in those nitrided without NiO, and it decreases further with increased nitridation temperature. This indicates that Si₃N₄ formation via gas phase reaction decreases with increasing temperature when NiO is present.

4.1. Nitridation of oxidized silicon powder

Preoxidation of high-surface-area attrition-milled powders delays the nitridation reaction and decreases the total conversion in 4-h nitridation at 1250 °C. The greater the degree of oxidation, the greater the retarding effect on nitridation kinetics. Results also show that when H₂ is added to N₂, the incubation time is reduced and nitridation is enhanced. From a practical point of view, this behavior suggests that even if a high-surface-area powder is mildly oxidized during aqueous slurry processing and consolidation, complete nitridation of the compact can be achieved.

Retardation of nitridation kinetics due to oxidation of laser synthesized high purity silicon powders has been reported by Sheldon and Haggerty [11]. They attributed the increased incubation period for nitridation to a decreased nucleation rate of Si₃N₄ with increasing oxidation. In this study, the retardation in a N₂ environment and enhancement in a N₂ + H₂ environment are probably related to nucleation and diffusion of N₂ through the silicate. It is hypothesized that because of oxidation, nucleation density decreases and N₂ diffusion through the silicate also decreases since viscosity is increased. In the presence of H₂, the thickness of the silica or silicate layer is reduced; thus the silicon is directly exposed to N₂ and nucleation is increased. Both favor enhanced nitridation. Another way to overcome the oxidation effects on nitridation kinetics is to add a nitride-enhancing additive, as the data shown in Fig. 9 suggest. From a practical point of view, these data are encouraging because, even if the high-surface-area

silicon powder were partially oxidized during slurry preparations, complete nitridation could be achieved at low temperatures, either by nitriding the compact in the presence of H₂ or by adding nitride-enhancing additives.

In summary, high-surface-area silicon powders can be prepared by attrition milling. However, prolonged attrition milling results in contamination of the silicon powder. Experiments indicate that a lower temperature, shorter duration nitridation cycle (suitable for processing RBSN composites reinforced by small diameter SiC fibers) can be developed by controlling the particle size and purity of the silicon powder. The RBSN material processed from relatively pure, submicron silicon powders from attrition milling contained large amounts of silica, Si₂N₂O, and β-Si₃N₄. Commercial RBSN material processing is optimized to achieve high amounts of α-Si₃N₄, which is known to improve the high-temperature properties of RBSN. The influence of silica and Si₂N₂O phases on the high-temperature properties of the RBSN fabricated in this study is not known and certainly warrants further investigation.

5. Summary of results

The surface area commercially available silicon powder was increased by wet attrition milling to facilitate processing and conversion to silicon nitride. The sensitivity of high-surface-area silicon powders to oxidation in air and under RBSN processing conditions was evaluated. The influences of surface area, polymer char, a nitride-enhancing additive, the nitridation environment, and preoxidation on the nitridation kinetics of the powder compacts were investigated. Key findings are as follows:

(1) Silicon powders that were attrition-milled in an inert solvent contained native silica and showed no tendency for further oxidation, even after exposure to air for a month or to deionized water for 4 days. However, these powders did oxidize after a 24-h exposure to acidic or basic solutions.

(2) At a given temperature, as the surface area of the silicon powder increased, so did the percent nitridation after 4 h, but the α/β ratio decreased. Silicon powders having a surface area of 40 m²/g or larger could be nitrided to 70-percent conversion or greater in 4 h at 1250 °C or above.

(3) Residual carbon char in, or preoxidation of, high-surface-area silicon powder delayed the start of the nitridation reaction, but the reaction did proceed to a significant degree.

(4) The nitridation environment had no significant influence on the nitridation kinetics of high-surface-area silicon powder compacts.

(5) At 1250 °C or greater, the addition of small amounts (0.4 to 0.6 wt %) of transition metal impurities, Ni or Fe, or both, was sufficient to completely nitride the compacts prepared from the high-surface-area silicon powder.

(6) Preoxidation of high-surface-area silicon powder compacts retarded nitridation kinetics. However, the

deleterious effects of oxidation could be avoided by nitriding the preoxidized compacts in an N₂-H₂ mixture or by adding nitride-enhancing additives.

(7) Devitrification of the silica layer by impurities, followed by the formation of a glassy phase due to the reaction of silica with the yttria and alumina impurities (from erosion of the grinding medium during attrition milling) and an increased density of nucleation with decreasing particle size were responsible for enhanced nitridation of high-surface-area powders.

6. Concluding remarks

High-surface-area silicon powders required for RBSN composite fabrication can be prepared by attrition milling commercially available silicon powders. However, during attrition milling, wear of the grinding medium invariably introduces impurities into the silicon powder. Although high-surface-area silicon powders do not show a tendency for further oxidation in ambient air, they do oxidize after prolonged exposure to aqueous acidic or basic solvents. This suggests that the aqueous based silicon slurries for RBSN processing may have a limited shelf life. However, by controlling the particle size of, and impurities in, the attrition-milled silicon powder, a low-temperature RBSN processing cycle that is cost effective, yields complete conversion of silicon to Si₃N₄, and is benign to commercially available small diameter SiC fibers can be developed for processing SiC/RBSN composites.

References

1. F. L. RILEY (ed.), "Nitrogen Ceramics" (Noordhoff, Leyden, 1977).
2. E. M. LENOE, R. N. KATZ and J. J. BURKE (eds.), "Ceramics for High Performance Applications," Vol. 3 (Plenum, New York, London, 1979).
3. A. J. MOULSON, *J. Mater. Sci.* **14** (1979) 1017.

4. J. A. MANGELS and G. J. TENNENHOUSE, *Bull. Amer. Ceram. Soc.* **59**(12) (1980) 1216.
5. O. J. GREGORY and M. H. RICHMAN, *J. Amer. Ceram. Soc.* **67** (1984) 335.
6. S. KLEBER and J. H. WEISS, *J. Eur. Ceram. Soc.* **10** (1992) 205.
7. R. T. BHATT, US Patent no. 4689188 (1987).
8. J. W. LUCEK, G. A. ROSSETTI, JR. and S. D. HARTLINE, in "Metal Matrix, Carbon, and Ceramic Matrix Composites," NASA CP-2406, edited by J. D. Buckley (NASA Lewis Research Center, Cleveland, OH, 1985) p. 27.
9. W. R. CANNON, S. C. DANFORTH, J. H. FLINT, J. S. HAGGERTY and R. A. MARRA, *J. Amer. Ceram. Soc.* **65**(7) (1982) 330.
10. T. P. HERBELL, T. K. GLASGOW and N. W. ORTH, *Bull. Amer. Ceram. Soc.* **63**(9) (1984) 1176.
11. B. W. SHELDON and J. S. HAGGERTY, *Ceram. Eng. Sci. Proc.* **9**(7/8) (1988) 1061.
12. R. G. PIGEON, A. VERMA and A. E. MILLER, *J. Mater. Sci.* **28** (1993) 1919.
13. M. BARSOUM, P. KANGUTKAR and M. J. KOZAK, *J. Amer. Ceram. Soc.* **76**(6) (1991) 1248.
14. R. V. GIRIDHAR and K. ROSE, *J. Electrochem. Soc.* **135**(11) (1988) 2803.
15. M. N. RAHAMAN and A. J. MOULSON, *J. Mater. Sci.* **19** (1984) 189.
16. J. A. MANGELS, *J. Amer. Ceram. Soc.* **58** (1975) 354.
17. S. M. BOYER and A. J. MOULSON, *ibid.* **13** (1978) 1637.
18. W. R. MOSER, D. S. BRIERE, R. C. CORRERIA and G. A. ROSSETTI, JR., *J. Mater. Res.* **1**(6) (1986) 797.
19. F. W. AINGER, *J. Mater. Sci.* **1** (1966) 1.
20. A. ATKINSON, A. J. MOULSON and E. W. ROBERTS, *J. Amer. Ceram. Soc.* **59** (1976) 285.
21. C. G. COFER and J. A. LEWIS, *J. Mater. Sci.* **29** (1994) 5880.
22. A. DE, S. JAYATILAKA and J. A. LEAKE, in "Nitrogen Ceramics," edited by F. L. Riley (Noordhoff, Leyden, 1977) p. 289.
23. H. M. JENNINGS, *J. Mater. Res.* **3** (1988) 907.
24. G. WOTTING and G. ZIEGLER, in "Proceedings of the 5th CIMTEC Conference," edited by P. Vincenzini (Elsevier, Amsterdam, 1983) p. 951.

Received 19 January

and accepted 4 November 1998